

# A High Strength Ti-SiC Metal Matrix Composite

K. M. Rahman<sup>a</sup>, V. A. Vorontsov<sup>a</sup>, S. M. Flitcroft<sup>b</sup>, D. Dye<sup>a</sup>

<sup>a</sup>Department of Materials, Royal School of Mines, Imperial College London, Prince Consort Road, London SW7 2BP, UK

<sup>b</sup>TISICS Ltd. 22 Invincible Road, Farnborough, Hampshire, GU14 7QU, UK

---

## Abstract

A SiC reinforced Ti-5Al-5Mo-5V-3Cr matrix metal matrix composite was developed. Monolithic blocks of alloy were hot rolled *via* pack rolling to produce foils for MMC panel fabrication. These were consolidated using hot isostatic pressing and solution treated and aged for optimum strength. The panels exhibited a strength of 2 GPa in tension and 3.5 GPa in compression, compared to the aerospace steel 300M, which has a tensile strength of 1.69 GPa. The fatigue performance of the material exceeded that of MMCs developed using Ti-21S or Ti-6Al-4V matrices. Finally, the reaction zone between the SiC and matrix was examined, revealing the presence of TiC.

*Key words:* Metal Matrix Composites, Fatigue, Strength, Mechanical Testing, Isostatic processing

---

## 1. Introduction

Metal matrix composites (MMCs) provide superior properties compared to monolithic materials, typically having higher strength and stiffness while reducing density [1]. MMCs generally exist in two forms: continuous fibre and particle reinforced composites. The former, although more expensive, provides the most effective strengthening in a specific direction [2]. Improvements in strength and stiffness, while reducing weight, allow dimensional and mass reductions in components. Thus, MMCs have received extensive research interest and are extremely attractive for industrial use [2–4].

A variety of MMCs have been developed utilising different reinforcement and matrix materials. Reinforcements are available in the form of continuous and short fibres, whiskers and particles, where continuous fibres have an aspect ratio approaching infinity [5]. MMC reinforcements range from carbon, boron, oxides *e.g.* alumina and non-oxides *e.g.* SiC. Some fibres have significant anisotropy, making polycrystalline fibres such as SiC attractive [6].

Titanium alloys combine light weight, high strength and good chemical resistance, leading to extensive use in engineering components [7, 8]. These attributes make titanium an excellent matrix material in MMCs. Although the most commonly used aerospace titanium alloy is the  $\alpha+\beta$  alloy Ti-6Al-4V [9–11], metastable  $\beta$  alloys such as Ti-5Al-5Mo-5V-3Cr offer significant improvements in strength ( $>1.4$  GPa) [12]. Metastable  $\beta$  alloys are able to maintain good properties throughout thick sections, *e.g.* for large components [13]. The lower  $\beta$  transus temperature in alloys such as Ti-5-5-5-3 ( $\sim 845^\circ\text{C}$ ) also enables processing at lower temperatures, reducing associated energy costs [14, 15]. In addition, Ti-5-5-5-3 has processing advantages over older high strength  $\beta$  alloys such as Ti-3Al-8V-6Cr-4Mo-4Zr (Beta-C). Beta-C is stronger than Ti-5-5-5-3 in the

cold rolled and aged condition where dislocations are used to nucleate fine  $\alpha$  precipitates. However, Ti-5-5-5-3 is stronger in the forged condition. Since Beta-C requires cold work to maximise strength, which is not feasible in the production of large components, the alloy is restricted to applications such as springs.

Several techniques exist for producing Ti-MMCs [16, 17], including; fibre-foil-fibre (FFF), matrix coated mono tape (MCM) and matrix coated fibre (MCF) methods. MCF is most commonly manufactured *via* physical vapour deposition (PVD) [18], depositing matrix material onto single fibres, which are then packed into arrays and consolidated by hot isostatic pressing (HIPing) or vacuum hot pressing to form the composite. This production route has the disadvantage of being expensive due to the need for molten metal. The FFF technique uses alternately stacked layers of matrix foil and fibre mat. The array is then consolidated to produce the MMC. Material produced using the FFF method will exhibit good tensile strength and fracture toughness, but suffers from microstructural heterogeneity, giving rise to poorer fatigue performance than MCF methods. The major drawback of the FFF method is the lack of availability of high quality matrix foil for most alloys.

The current study investigates the benefit of using a Ti-5-5-5-3 matrix in a SiC fibre reinforced MMC. The overriding objective is to develop the strongest MMC possible, utilising feasible processing routes. Monolithic matrix material was pack rolled to produce foil to consolidate with SiC fibres to form the MMC. A range of heat treatments were employed to maximise mechanical properties. In addition, microscopy was conducted to augment the results.

## 2. Experimental Procedures

Matrix foil was produced from Ti-5-5-5-3 blocks that were vacuum encapsulated within a 20x100x60 mm steel frame. These blocks were hot rolled at 810 °C, to a final reduction of 90%. A 5 min interpass time was used for reheating the billet. Once rolled the steel frame was evacuated, the titanium was sectioned, coated in yttria, re-stacked and encapsulated for further rolling, until foil with a nominal thickness of 140 µm was obtained.

The silicon carbide fibre used in this investigation was supplied by TISICS Limited, variant SM3156, which had a nominal fibre diameter of 140 µm with a minimum strength of 3.8 GPa.

The FFF approach was used to consolidate MMC panels *via* HIPing at 840 °C for 5 h. The panels were manufactured with a 39% fibre volume fraction ( $V_f$ ) and had a thickness of 5 mm.

Samples for mechanical testing were produced using electric discharge machining. 10 mm wide strips were produced for tensile testing and 4x4x5 mm blocks for compression. Testing was conducted on a Zwick Roell 100 kN load frame at a nominal strain rate of  $1 \times 10^{-4} \text{ s}^{-1}$ . Fatigue testing was conducted using sinusoidal loading at an R ratio of 0.1 and a frequency of 5 Hz under a maximum applied stress ranging between 40-75% of the tensile strength. Loading was applied parallel to the fibre direction for all the mechanical testing. Tensile testing was conducted on 6 specimens to account for scatter, similarly 3 samples were tested in compression and 3 samples were tested in fatigue for each maximum applied stress.

Samples for transmission electron microscopy were prepared using Focussed Ion Beam (FIB) milling on a FEI Helios NanoLab 600 series Dual Beam microscope. Electron backscatter diffraction (EBSD) and imaging was conducted on a Zeiss Auriga FEGSEM equipped with a Bruker EBSD system. Scanning transmission electron microscopy (STEM) was conducted on a JEOL JEM-2100F microscope.

## 3. Results and Discussion

The microstructure of the Ti-5-5-5-3 prior to rolling is shown in Figure 1. A coarse  $\beta$  grain size of  $\sim 200 \mu\text{m}$  was observed, with globular primary  $\alpha$  precipitates  $\sim 4 \mu\text{m}$  in size. This type of microstructure is usually obtained after sufficient  $\alpha + \beta$  processing followed by a solution treatment in the  $\alpha + \beta$  region [19]. In addition, fine acicular secondary  $\alpha$  laths ranging between 50 to 200 nm were observed, Figure 1(b-d). This morphology results from nucleation and growth transformation of  $\beta$  to  $\alpha$  where the  $\alpha$  nucleates and grows on preferred crystallographic planes of the parent  $\beta$  phase [20]. Acicular laths were observed decorating the  $\beta$  grain boundaries with some finer  $\alpha$  laths originating and growing towards the centre of the grain.

EBSD maps with inverse pole figure (IPF) colouring parallel to the forging direction is shown in Figure 1(c-f).

Examination of the  $\{0001\}$   $\alpha$  and  $\{110\}$   $\beta$  pole figures, suggested that the  $\beta$  to  $\alpha$  phase transformation followed the expected Burgers orientation relationship;  $\{110\}_\beta // \{0001\}_\alpha$  and  $\langle 111 \rangle_\beta // \langle 2\bar{1}10 \rangle_\alpha$ .

Test MMC panels composing of a 5-ply layup were fabricated and an essentially defect-free microstructure was observed. Pores were not observed between foil layers and excellent wetting between the SiC and matrix was found. The matrix material formed a continuous bond with the C layer coating the SiC, Figure 2(c).

Figure 2(e-f) shows the microstructure observed when HIPed above the  $\beta$  transus. Here, large  $\beta$  grains can be seen interlinking the fibres, with grain boundary  $\alpha$  often found nearly continuously linking the fibres. In titanium alloys, such grain boundary  $\alpha$  is typically found to result in inferior ductility and fatigue strength [21]. In addition, a line between the matrix layers can be seen in Figure 2(f) which is due to the incomplete bonding between the individual matrix foils. These defects were not observed in the sub-transus MMC panels.

The ductility of a MMC is limited by that of the fibre. Therefore, for the purposes of maximising strength, the MMC panels were solution treated and aged (STA) to increase the matrix strength. The panels were solution treated at 840 °C for 30 min followed by air cooling, aged at 580 °C for 8 h and then air cooled again. This resulted in a microstructure composed of fewer globular primary  $\alpha$ ,  $\sim 2 \mu\text{m}$  in size and a large fraction of  $< 20 \text{ nm}$  fine secondary  $\alpha$  laths for strengthening, Figure 2(c-d).

Heat treating close to the  $\beta$  transus results in a lower fraction of primary  $\alpha$ , which does not significantly contribute to improving strength. This also means that a higher concentration of  $\alpha$  stabilisers, *e.g.* Al, remain in solution that are available to precipitate fine scale secondary  $\alpha$  laths during ageing. Fanning *et al.* [12, 21, 22] have reported peak tensile strengths in Ti-5-5-5-3 of 850-950 MPa in the solutionised condition, which increases to

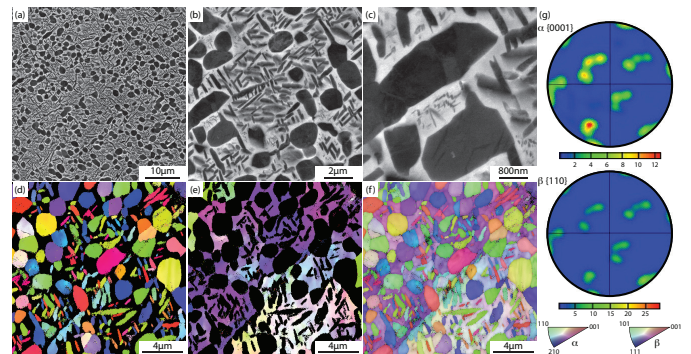


Figure 1: Initial microstructure of the Ti-5553 matrix material showing (a) distribution of globular primary alpha, (b,c) with fine secondary acicular alpha, (d) EBSD map of the hexagonal alpha phase with inverse pole figure (IPF) colouring (e) IPF coloured map of the cubic beta phase, (f) IPF coloured map of the microstructure composed of both alpha and beta and (g) alpha  $\{0001\}$  and beta  $\{110\}$  poles figures. IPF colouring is referred to the sample surface normal.

159  $\sim 1400$  MPa once aged. Higher strengths were reported  
 160 when the material was aged at lower temperatures, *i.e.*  
 161  $560$ - $680$  °C. This is due to the formation of finer  $\alpha$  laths  
 162 which provide more interfaces and increase strength. How-  
 163 ever, low temperature ageing has a detrimental effect on  
 164 ductility and toughness. When considering application in  
 165 a MMC these shortcomings can be negated. Firstly, the  
 166 ductility of the MMC will be dictated by the fibre. Finally,  
 167 toughness and resistance to crack growth will be enhanced  
 168 due to the extensive crack bridging facilitated by unbroken  
 169 fibres [23].

170 An interfacial reaction zone less than  $1\ \mu\text{m}$  in thick-  
 171 ness arising from the reaction between the carbon layer  
 172 and the Ti-5-5-5-3 matrix during fabrication of the MMC<sup>176</sup>  
 173 was observed, Figure 3. A TEM foil was lifted out from<sup>177</sup>  
 174 the region and imaged. Energy Dispersive X-ray Spec-<sup>178</sup>  
 175 troscopy (EDS) was used to collect elemental maps from<sup>179</sup>

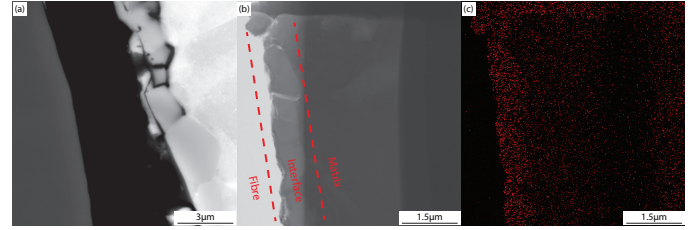


Figure 3: Interfacial reaction zone between carbon layer surrounding SiC and titanium matrix imaged using (a) secondary electron imaging, (b) bright field TEM and (c) corresponding carbon EDS map (K $\alpha$ 1).

180

the region to visualise chemical segregation. The element mapping clearly illustrates the formation of TiC in the reaction zone. Fu *et al.* [28] have reported the formation of TiC in a Ti-6-4 - SiC MMC, while Huang *et al.* [29] have reported the presence of a Ti<sub>5</sub>Si<sub>3</sub> layer also in a Ti-6-4 - SiC MMC. The current investigation found no evidence of a distinct phase in the reaction zone in the present case.

The mechanical performance of the MMC panels was tested in both compression and tension, Table 1. The tensile strength was  $\sim 2$  GPa with an elastic modulus of 200 GPa. Similarly the strength in compression was found to be  $\sim 3.5$  GPa. These properties are superior to similar MMCs reported in the literature including Ti and Al matrix composites [24, 25]. Baik [25] has reported a tensile strength of 1.2 GPa in a Ti-6-4/SiC reinforced composite, which is significantly lower than the current study even after considering differences in fibre  $V_f$ . A Ti-21S (Ti-15Mo-3Nb-3Al-0.2Si - metastable  $\beta$  alloy) MMC panel was also produced during the present study for comparison; the Ti-5-5-5-3 MMC was found to be  $\sim 350$  MPa stronger in tension. This is most likely because the dislocation content required for Ti-21S to precipitate fine scale  $\alpha$  during ageing cannot be retained through the HIP cycle; the ability of Ti-5-5-5-3 to produce fine scale  $\alpha$  after hot working is the reason for selection of this alloy as the matrix material. In addition, Table 2 compares the strength of MMCs consolidated using various Ti matrix alloys by the authors, which have been normalised for a 33%  $V_f$ . Here, it can clearly be seen that Ti-5-5-5-3 results in the highest strength yet attained in this system, with a density  $\rho = 3.90\ \text{g cm}^{-3}$ . Although, the alloy Beta-C attains a similar tensile strength, this can only be achieved in the cold rolled and aged condition which is not suitable for most engineering applications. For many aerospace structures of interest, Ti-MMCs would substitute for a martensitic steel such as 300M, which has a density  $\rho = 7.87\ \text{g cm}^{-3}$ , a yield strength of 1690 MPa and also requires corrosion-resistant coating with Cd-containing paints. Therefore the specific strength of the present Ti-MMC is approximately 2.4 times greater, with 39%  $V_f$ .

The fatigue behaviour of the Ti-5-5-5-3 MMC compared to Ti-21S matrix panels is shown in Figure 4. The peak stress was selected at increasing proportions of the tensile stress, ranging from 40-75% (800-1500 MPa). The

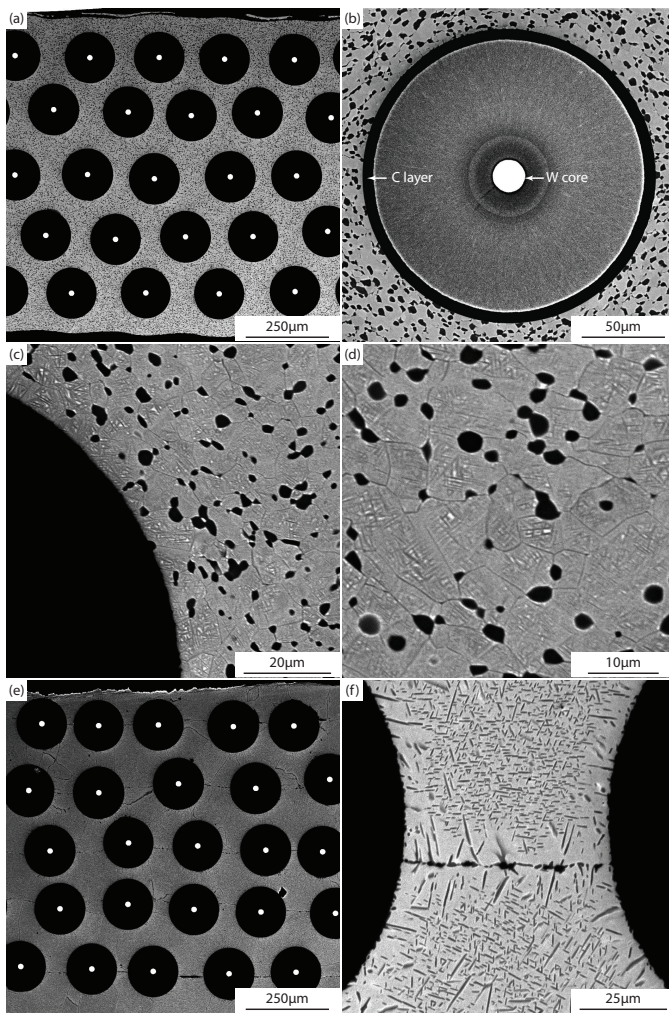


Figure 2: (a-d) Microstructure of a 5-ply MMC panel HIPed at  $840^\circ\text{C}$ <sup>214</sup> showing (a) overview of the matrix and fibres, (b) interaction be-<sup>215</sup> tween SiC fibre and matrix Ti-5553. The W core and C layer around<sup>216</sup> the SiC is also observed (image has been composited in order to man-<sup>217</sup> age the contrast between the fibre and matrix), (c) globular primary<sup>218</sup> alpha for retarding grain growth and (d) fine scale secondary alpha<sup>219</sup> for strengthening. (e-f) Panel HIPed at  $910^\circ\text{C}$ , above the  $\beta$  transus.<sup>219</sup>



Table 1: Mechanical properties of the MMC panel tested in tension and compression.

Test Mode	Stiffness	Max. Stress	Failure Strain
	GPa	MPa	%
Tension	200	2050 ± 110	1.0
Compression	-	3500 ± 60	0.8

Table 2: Comparison of the tensile strength of various Ti matrix MMCs normalised for a 33% volume fraction ( $V_f$ ) of fibres. SiC fibres used were from TISICS Limited, variant SM1140+, 100  $\mu$ m diameter, minimum strength 3.5GPa. \*Beta-C strength calculated using a rule of mixtures method.

Matrix	Tensile Strength MPa
Ti-6V-4Al	1620
Ti-15V-3Sn-3Cr-3Al	1610
Ti-15Mo-3Nb-3Al-0.2Si (Ti-21S)	1625
Ti-6Al-2Sn-4Zr-2Mo	1635
Ti-5Al-5Mo-5V-3Cr (super transus)	1820
Ti-5Al-5Mo-5V-3Cr (sub transus)	1920
Ti-3Al-8V-6Cr-4Mo-4Zr (Beta-C)*	1920

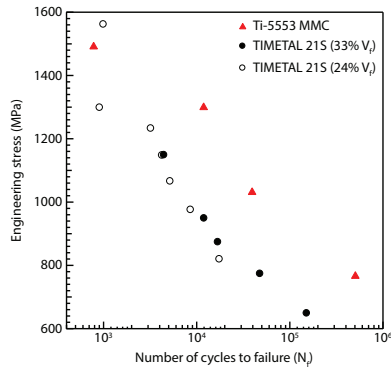


Figure 4: Fatigue properties of the MMC panel compared to Ti-21S which had a tensile strength of  $\sim 1.6$  GPa.

performance of the Ti-5-5-5-3 MMC in fatigue was found to be approximately 200 MPa (25%) higher at a life of  $10^5$  cycles compared to the MMC with a TIMETAL 21S matrix. Ti-5-5-5-3 achieved in excess of 550,000 cycles before failure at 800 MPa. The fatigue life was found to be superior to other Ti MMCs reported in literature, including Ti-6-4 and Ti-15-3-3-3 matrix composites [26, 27].

The fracture surface of the tensile test specimen is shown in Figure 5. A classic MMC fracture surface is observed with evidence of fibre pull out during loading, Figure 5(a), along with evidence of cleavage occurring in the brittle SiC fibres, Figure 5(b). Conversely, the matrix exhibits characteristics of ductile failure due to the presence of numerous voids and the observation of void coalescence. Evidence of fibre pull out indicates that catastrophic failure of the fibres did not occur. Thus load is transferred from the matrix onto the fibres during tensile loading accounting for the higher strength to failure of the composite.

Figure 6 shows the fracture surface of the sample which

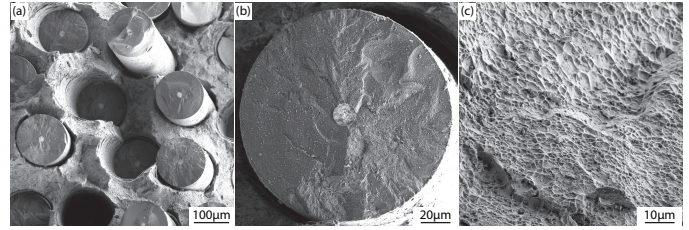


Figure 5: Fracture surface of the tensile test specimen exhibiting (a) fibre pull out, (b) cleavage of the brittle silicon carbide reinforcement and (c) void coalescence indicating ductile failure of the Ti-5-5-5-3 matrix.

was tested to a peak stress of 800 MPa and accumulated an excess of 550,000 cycles before failure. The surface reveals the presence of ledges, Figure 6(a), which results from crack deflection during loading. The boundary of these ledges is decorated with fibres that have undergone pull out and are most likely due to either localised bending, shear or compression of the fibres on the ledge. Examination of the fracture surface suggests that the initiation point for failure originated at the SiC fibres that were located on the edge of the test specimen, Figure 6(b). During loading these fibres were cleaved, resulting in the appearance of planar facets in the matrix surrounding the fibre, Figure 6(c). Away from the initiation surface the matrix exhibits striations and the presence of void coalescence in the central region of the specimen, Figure 6(d,e).

## 4. Conclusions

In summary, a Ti-5-5-5-3 - SiC reinforced MMC was developed using a combination of pack rolling to produce metal foil, and a foil-fibre-foil layup method. The forged Ti-5-5-5-3 used in hot rolling was composed of globular primary  $\alpha$  precipitates coupled with  $<50$  nm acicular secondary  $\alpha$  laths. The texture was typical for a forged component exhibiting a Burgers type orientation relationship. The reaction zone between the fibre and matrix revealed a TiC layer. The MMC panels were solution treated and aged to optimise strength. This resulted in a 2 GPa tensile strength and 3.5 GPa flow stress in compression. The fatigue properties were excellent, requiring an excess of 550,000 cycles before failure at 800 MPa.

## 5. Acknowledgements

The authors would like to thank R. P. Durman and S. Kyle-Henney from TISICS Limited, Farnborough, UK, for material supply and production of the MMC panels. This work was part-funded by the Technology Strategy Board under grant TS/L000288/1 131238.

## References

- [1] N. Chawla, Y.-L. Shen, *Adv. Eng. Mater.* **2001**, *3*, 357.

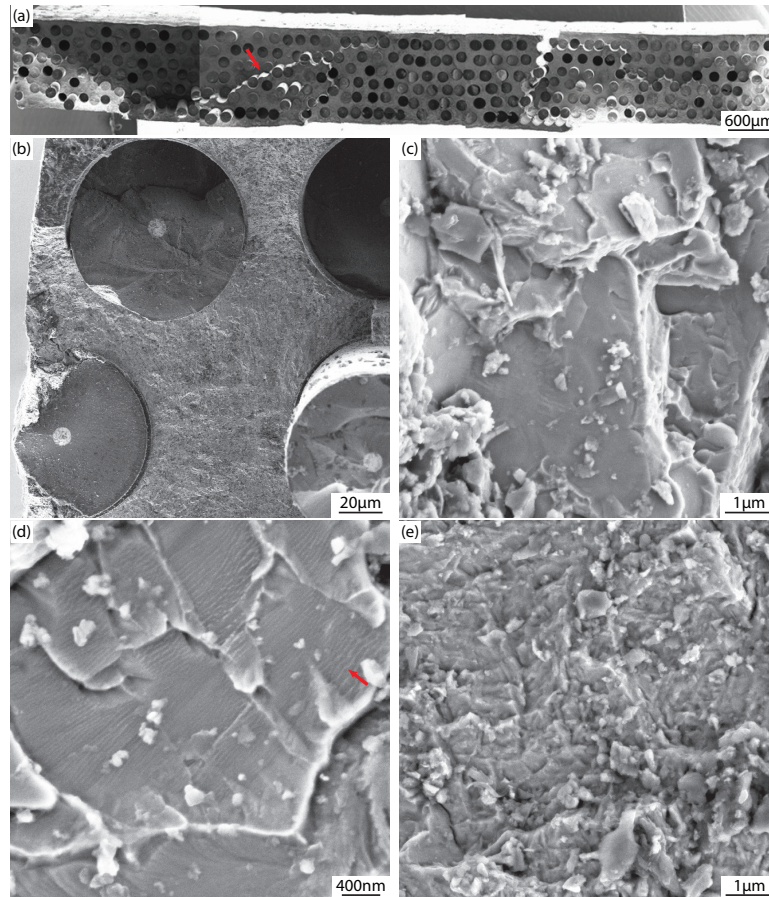


Figure 6: Fracture surface of specimen fatigue tested to a peak stress of 800 MPa showing (a) overview of the sample (arrow indicates ledges), (b) cleavage of the brittle silicon carbide reinforcement with the suspected initiation region, (c) planar facets located near the fibres, (d) striations further into the sample (indicated with arrow) and (e) void coalescence.

- 277 [2] S.R. Bakshi, D. Lahiri, A. Agarwal, *Int. Mater. Rev.* **2010**, *55*,306  
278 41. 307
- 279 [3] S. Rawal, *J. Mater.* **2001**, 14. 308
- 280 [4] N. Takahashi, T. Sato, S. Nakatsuka, K. Fujiwara, K. Yoshida,309  
281 T. Yokozeki, *Int. Congr. Aeronaut. Sci.* **2012**, *1*, 1. 310
- 282 [5] A. Mortensen, J. Llorca, *Annu. Rev. Mater. Res.* **2010**, *40*,311  
283 243. 312
- 284 [6] N. Chawla, K.K. Chawla, *Metal Matrix Composites*, 2nd Edi-313  
285 tion, Springer, **2014**. 314
- 286 [7] R. Boyer, R. Briggs, *J. Mater. Eng. Perform.* **2005**, *14*, 681. 315
- 287 [8] M. Peters, J. Kumpfert, C. Ward, C. Leyens, *Adv. Eng. Mater.*316  
288 **2003**, *5*, 419. 317
- 289 [9] S. L. Semiatin, V. Seetharaman, A. K. Ghosh, *Philos. Trans.*318  
290 *R. Soc. A: Math. Phys. Eng. Sci.* **1999**, *357*, 1487. 319
- 291 [10] S. L. Semiatin, T. R. Bieler, *Acta. Mater.* **2001**, *49*, 3565. 320
- 292 [11] A. K. Jha, S. K. Singh, M. S. Kiranmayee, K. Sreekumar,321  
293 P. Sinha, *Eng. Fail. Anal.* **2010**, *17*, 1457. 322
- 294 [12] J. Fanning, *J. Mater. Eng.* **2005**, *14*, 788. 323
- 295 [13] N. G. Jones, M. Jackson, *Mater. Sci. Tech.* **2011**, *27*, 1025. 324
- 296 [14] N. G. Jones, R. Dashwood, D. Dye, M. Jackson, *Metall. Mater.*  
297 *Trans.* **2009**, *40*, 1944.
- 298 [15] N. G. Jones, R. Dashwood, M. Jackson, D. Dye, *Acta. Mater.*  
299 **2009**, *57*, 3830.
- 300 [16] Z. X. Guo, B. Derby, *Prog. Mater. Sci.* **1995**, 411.
- 301 [17] C. M. Lobley, Z. X. Guo, *Mater. Sci. Tech.* **1998**, *14*, 1024.
- 302 [18] H. X. Peng, *J. Mater. Sci. Tech.* **2005**, *21*, 647.
- 303 [19] S. Shekhar, R. Sarkar, S. K. Kar, A. Bhattacharjee, *Mater.*  
304 *Des.* **2015**, *66*, 596.
- 305 [20] F. H. Froes *Titanium: Physical Metallurgy, Processing, and*  
*Applications*, ASM International, **2015**.
- [21] J. Fanning, R. Boyer, *World Conference on Titanium.* **2003**,  
*1*, 2643.
- [22] J. Fanning, S. L. Nyakana, K. M. Patterson, R. C. McDaniel,  
*Ti-2007 Sci. Tech.* **2007**, *1*, 499.
- [23] D. L. Davidson Southwest Research Institute, San Antonio,  
TX,**1989**, 1.
- [24] P. Ashwath, M. A. Xavior, Processing methods and property  
evaluation of Al<sub>2</sub>O<sub>3</sub> and SiC reinforced metal matrix composites  
based on aluminium 2xxx alloys. *J. Mater. Res.* 2016;*31*:1201-  
1219. *J. Mater. Res.* **2016**, *31*, 1201.
- [25] K. H. Baik *Mater. Trans.* **2006**, *47*, 2815.
- [26] B. Lerch, G. Halford, *Mater. Sci. Eng. A.* **1995**, *200*, 47.
- [27] B. P. Sanders, S. Mall, R. B. Pittman, *Composites Sci. Tech.*  
**1999**, *59*, 583.
- [28] Y. Fu, N. Shi, D. Zhang, R. Yang, *Mater. Sci. Eng. A.* **2006**,  
*426*, 278.
- [29] B. Huang, M. Li, Y. Chen, X. Luo, Y. Yang, *Mater. Charact.*  
**2015**, *109*, 206.